Bayesian Optimization Framework for Multi-Objective Charging Strategy Design in Lithium-Ion Batteries

Rashi Verma
Department of Chemical Engineering, Indian Institute of Technology,Hyderabad
Hyderabad, India
ch22resch11004@iith.ac.in

Suryanarayana Kolluri
Department of Chemical Engineering
University of Washington, Seattle
Washington, USA
kolluri.suryanarayana@gmail.com

Kishalay Mitra*
Department of Chemical Engineering, Indian Institute of Technology,Hyderabad
Hyderabad, India
kishalay@che.iith.ac.in

***Abstract*— Lithium-ion batteries (LIBs) underpin modern electrification, enabling applications ranging from portable electronics and electric vehicles to grid-scale energy storage systems. However, their large-scale deployment is constrained by critical safety concerns, including thermal runaway, alongside performance-degrading phenomena such as lithium plating, capacity fade, and irreversible aging. To overcome these limitations, there is a pressing need to move beyond empirical, trial-and-error based charging protocols toward rigorous optimization frameworks that ensure fast, safe charging while extending battery life. In this work, a high-fidelity, physics-based single-particle electrochemical-thermal model with electrolyte and thermal coupling (SPMeT) is used. This mechanistic modelling framework is integrated within a multi-objective Bayesian optimization algorithm. This scheme is designed to systematically explore and optimize charging protocols. Findings show that Multi-Objective Bayesian Optimization (MOBO) requires only 2.06% of the function calls required by NSGA-II, a well-established and popularly used multi-objective evolutionary algorithm, to achieve similar quality of solutions highlighting its lower computational cost. The proposed approach identifies Pareto-optimal charging strategies that balance charging time, thermal stability, and stored energy, thus providing practically relevant solutions for real-world lithium-ion battery operation at lower computational cost.**

Keywords—Bayesian Optimization, Multi-Objective Optimization, Single Particle Model, Optimal charging strategy, multi-stage constant current

I. INTRODUCTION

To address the urgent challenges of the global energy crisis and environmental pollution, many countries are vigorously advancing new energy technologies. Among these, electric vehicles (EVs) stand out as a prominent innovation due to their superior energy efficiency and potential to mitigate environmental issues such as emissions, fossil fuel dependence, and air pollution. Central to the functionality of EVs is the battery pack, which serves as the primary energy source. Lithium-ion (Li-ion) batteries have emerged as the preferred choice for modern energy storage in EVs and grid applications, owing to their high gravimetric energy density (~100 Wh/kg), substantial power density (~300 W/kg) [1], wide operational temperature range, and extended cycle life. Even with these benefits, Li-ion batteries can still lose capacity to degradation and pose safety risks because of thermal runaway. To overcome these challenges, we require better charging protocols that not only allow for quick charging but also protect the health of the battery for the user's convenience and extend the battery's long life.
The results reported in this paper are reproducible through the use of the open-source libraries **PyBaMM**, **BoTorch**, and **pymoo**.

II. RELATED WORK

In the literature, various conventional charging protocols have been reported to charge any battery that includes standard constant current–constant voltage (CC–CV), pulse charging, and multi-stage constant current (MSCC) [2]. Each protocols exhibits its own distinct trade-offs in terms of implementation complexity and achievable charging time. These pre-defined charging strategies help in developing optimal charging strategy by using various types of models e.g. equivalent circuit model (ECM) or detailed physics based model e.g. Single Particle Model (SPM)[3], SPMe[4], Pseudo-2-Dimension (P2D) Model [5]. For instance Zhang *et al.*, 2014 [6] conducted an optimization study using a genetic algorithm based on ECM model to study how adapting charging current with respect to state of charge and cycle can enhance the battery charging efficiency and achieve longer life. Similarly, in [7], a dynamic optimization framework based on ECM was employed to develop optimal charging strategy by exploiting the conflicting trade-offs between charging time and capacity loss as primary objectives. Likewise in [8], a plug-in hybrid electric vehicle model was considered to perform multi-objectives optimization of charging strategy by considering the energy cost and battery life as primary objectives. Similarly, a single objective optimization problem was solved using BO on porous electrode theory-based model to design a fast charging protocol [9] . In a comparable study, a multi-objective optimization was performed for developing an optimal charging profile by considering charging time, energy loss and temperature increase as objectives, and using a simplified equivalent circuit model [10]. Zhu et al in [11] proposed a data-driven model for solving a multi-objective optimization problem using MOBO algorithm by considering knee point capacity

* Corresponding author

and cycle life as key objectives. In the existing literature, most studies on battery charging optimization predominantly rely on single-objective formulations, simplified empirical models or data-based model, typically solved using classical control or conventional optimization techniques. Such approaches generally overlook the conflicting nature of multiple performance indicators and lack the ability to exploit high-fidelity electrochemical representations of lithium-ion batteries.

To address these limitations, the present work employs a multi-objective Bayesian Optimization (MOBO) framework integrated with a physics-based electrochemical–thermal model, namely the Single Particle Model with Electrolyte and Thermal Dynamics (SPMeT). In the proposed framework, Gaussian Process Regression (GPR) surrogate models iteratively approximate the objective and constraint functions from high-fidelity simulations, while the q-Expected Hypervolume Improvement (q-EHVI) acquisition function integrated with probabilistic constraint handling efficiently selects new charging strategies that balance exploration, exploitation, and thermal safety compliance throughout the optimization. The current work proposes a multi-objective optimization framework for the multi-stage constant-current (MSCC) charging protocol, aimed at minimizing total charging time, temperature and maximizing charge stored, subject to stringent constraints on degradation metrics, including lithium plating risk, thermal runaway potential, and capacity fade.

The remainder of this paper is structured as follows: Section III introduces the SPMeT model and the formulation of the multi-objective optimization problem. Section IV describes the proposed MOBO-based methodology in detail. Section V presents the optimization results and discusses the Pareto-optimal charging strategies. Finally, Section VI concludes the study with key findings and research insights.

III. Methodology

A. Model description: Single Particle Model with Electrolyte and Thermal dynamics

The Single Particle Model with Electrolyte and Thermal dynamics (SPMeT) is a physics-based continuum electrochemical model that represents the solid-phase electrode particles in both the cathode and anode regions as single spherical particles. The model assumes, the mass and charge balances of these particles as volume-averaged across the electrode thickness, allowing the complex electrode behaviour to be captured in a computationally efficient manner while incorporating electrolyte transport and thermal effects. Model is governed by Fick's second law and Butler Volmer Kinetics[3]. The model is represented by two PDEs for lithium and charge balance in solid phase, three PDEs for electrolyte concentration and another three PDEs for electrolyte charge balance in three regions (anode, cathode and separator)

Solid-Phase Lithium diffusion equations:

$$\frac{\partial C_{s,k}}{\partial t} = -\frac{D_{s,k}}{r^2}\frac{\partial}{\partial r}\left(r^2\frac{\partial C_{s,k}}{\partial r}\right) \quad (1)$$

where, $C_{s,j}$ is lithium-ion concentration in electrodes k ϵ {n, p} where is used to represent negative, separator and positive electrode respectively and r ϵ [0, R_k]. $D_{s,k}$ is the diffusion coefficient in solid phase electrode particles.

Solid-Phase Charge transport equations:

$$\frac{\partial}{\partial x}\left(\sigma_{eff}\frac{\partial \Phi_{\{s,k\}}}{\partial t}\right) = -a_k F j \quad (2)$$

where σ_{eff} is the effective electronic conductivity in solid particle and a_k is the interfacial surface area of the electrode material and j is interfacial current density.

Electrolyte-Phase Lithium diffusion equations:

$$\epsilon_j \frac{\partial C_{s,k}}{\partial t} = -\frac{\partial N_{e,k}}{\partial x} + \begin{cases} \frac{I}{F L_n}, & k = n \\ 0, & k = s \\ -\frac{I}{F L_p}, & k = p \end{cases} \quad (3)$$

$$N_{e,k} = -\epsilon_j^b D_e \frac{\partial c_{e,k}}{\partial x} + \begin{cases} \frac{x\, t^+ IRT}{F L_n}, & k = n \\ \frac{t^+ IRT}{F}, & k = s \\ \frac{(1-x) t^+ IRT}{F L_p}, & k = p \end{cases} \quad (4)$$

where D_e is diffusion coefficient in electrolyte, $N_{e,j}$ stands for lithium-ion flux within k region where k ϵ{n,s,p} and x ϵ [0, L] is the macroscopic through-cell distance.

Electrolyte-Phase Charge transport equations:

Charge balance in the electrolyte phase is balanced by the following governing equations

$$\frac{\partial}{\partial x}\left(k_{eff}\frac{\partial \Phi_e}{\partial x}\right) + \frac{2RT}{F}(1 - t_+^o)\frac{\partial}{\partial x}\left(k_{D,eff}\frac{\partial \ln c_e}{\partial x}\right) + a_k F j = 0 \quad (5)$$

where, Φ_e is the electrolyte potential, k_{eff} is the effective ionic conductivity and $k_{D,eff}$ is the diffusional conductivity.

Kinetic equation: Butler-Volmer Equation

$$J_i = k_k\, c_{s,k,max} c_e^{\alpha_{a,k}} (1 - x_{k,surf})^{\alpha_{a,k}} x_{k,surf}^{\alpha_{c,k}} \left[exp\left(\frac{\alpha_{a,k} F}{RT} n_k\right) - exp\left(-\frac{\alpha_{c,k} F}{RT} n_k\right)\right] \quad (6)$$

where, $x_{k,surf} = \frac{c_{s,k}}{c_{s,k,max}}$, $x_k = \frac{c_{s,k}}{c_{s,k,max}}$, $k = \{n, p\}$

$$V_{cell} = \Phi s, p - \phi s, n \quad (7)$$

where, J_i stands for current density, F is Faraday's constant, R is Universal gas constant, V_{cell} is cell potential.

Thermal Model: Lumped Model

The lumped thermal model was coupled with the Single Particle Model with electrolyte to capture the cell's thermal behavior. The resulting equation was expressed as ordinary differential equation as shown in (Eq.8)

$$\rho_{eff}\frac{\partial T}{\partial t} = \bar{Q} - \frac{hA}{V}(T - T_\infty) \quad (8)$$

where, ρeff is effective volumetric heat capacity, T is the average temperature of the cell, h is the heat transfer

coefficient, $\bar{Q}$ is the averaged heat source A is the surface area, V is the cell volume and T_∞ the ambient temperature.

B. Multi-Objective Optimization Problem Formulation (MOOP)

A multi-objective framework was formulated to develop charging protocols that simultaneously minimize the total charging time, cell temperature, while maximizing the stored charge capacity. This formulation ensures rapid charging without compromising the thermal stability and cell integrity, subjected to certain physical constraints as mentioned in (Eq.10) - (Eq.11)

$$Minimize: F(x) = \begin{cases} f_1(x) = t_{time} \\ f_2(x) = -Q_{charge} \\ f_3(x) = T_{temp} \end{cases} \quad (9)$$

subject to solution of SPMeT Model: **Eq.1-8**

Constraints: $g_1(x) = 298\,K \leq T \leq 323$ K (10)

$$g_2(x) = V_{anode} \geq 0 \quad (11)$$

$x \in [C1, C2], \forall = Ci \in [C_{i,min}, C_{i,max}]$

Here x denotes the decision vector x= [C1, C2], Ci represent the charging rate, C rate of i^{th} stage. To avoid the Lithium plating, a constraint on anode plating overpotential (V_{anode}), which is considered as the difference between negative electrode in solid phase and electrolyte potential at anode/separator interface, is enforced to remain above 0 V vs. Li/Li^+. Furthermore, temperature limit was enforced to avoid any kind of thermal degradation of electrolyte and causing unfavorable and unsafe condition inside the battery. For simulating the electrochemical SPMeT model, the parameters by Okane et.al 2022 was adopted, as summarized in Table I.

TABLE I. LIST OF PARAMETERS

Parameter	Unit	Values
Initial concentration in electrolyte	$[mol.m^{-3}]$	1000.0
Initial concentration in negative electrode	$[mol.m^{-3}]$	29866.0
Initial concentration in positive electrode	$[mol.m^{-3}]$	17038.0
Positive electrode conductivity	$[S.m^{-1}]$	0.18
Negative electrode conductivity	$[S.m^{-1}]$	215.0
Negative particle radius	$[m]$	5.86e-06
Positive particle radius	$[m]$	5.22e-06
Electrode reaction anodic/Cathodic	–	0.5
Nominal cell capacity	$[A.h]$	5.0

IV. OPTIMIZATION TECHNIQUE

A. Multi-Objective Bayesian Optimization (MOBO)

Bayesian Optimization (BO) is an effective approach for addressing optimization problems involving computationally expensive objective functions. It falls under the category of surrogate-based optimization methods, where a surrogate model is constructed using Bayesian probabilistic frameworks to manage the trade-off between exploration and exploitation. The core components of BO include a stochastic surrogate model, commonly implemented as a Gaussian Process Regressor (GPR), that approximates the high-fidelity, time-consuming physics-based model, and an acquisition function derived from this surrogate to determine the most promising location for the next evaluation.

From an initial set of design points, a probabilistic surrogate model is constructed and used, together with a selected acquisition criterion, to determine the location of subsequent function evaluations. In standard Bayesian optimization settings, this surrogate is most commonly formulated as a Gaussian Process Regressor (GPR), which approximates the underlying objective function using the available observations. As additional evaluations are performed, the surrogate is updated sequentially, thereby refining both its mean response and associated predictive uncertainty. The acquisition function then steers the search process by indicating where the next evaluation should be carried out, balancing potential improvement in the objective against epistemic uncertainty. As a result, new samples are drawn either in regions already identified as promising, where the predicted objective values are high (exploitation), or in sparsely explored areas in which the surrogate exhibits large uncertainty (exploration) [12]. This loop is repeated until the evaluation budget is reached, that is, until the maximum allowed number of function calls has been used. In multi-objective Bayesian optimization (MOBO), a Gaussian Process Regression (GPR) surrogate constructed in this way tends to have limited ability to generalize over the whole design space, because it is fitted only to the small, task-specific set of samples generated during a given MOBO campaign, rather than to a large, diverse dataset as in conventional data-driven models. As a result, the GPR surrogate needs to be retrained whenever the operating conditions or problem setup change. A key advantage of this framework is that it can be directly applied to experimental studies, where expensive first-principles simulations are simply replaced by physical experiments performed at the design points proposed by the acquisition function, enabling efficient use of restricted experimental resources.

In single-objective optimization scenarios, acquisition functions such as Probability of Improvement, Upper Confidence Bound, and Expected Improvement are commonly employed. In case of multi-objective optimization problems with conflicting objective functions, identifying the trade-off solution become crucial, which is commonly referred to as nondominated or Pareto solutions In order to identify such solution with balanced trade-off we have considered the Expected Hypervolume Improvement (EHVI) acquisition function [13]. EHVI measures the improvement in hypervolume with respect to reference point, which serves as convergence indicator of Pareto front. Due to the inherent stochasticity in objective predictions from the probabilistic model, the EHVI is defined as the expected value of hypervolume improvement calculated over the Gaussian Process posterior distribution of the objectives to generate high quality Pareto-front. To calculate the Expected Hypervolume Improvement (EHVI) for multivariate probability density function generated by a surrogate model Gaussian Process Regression we use (Eq. 12) as in [14] .

$$EHVI(\mu, \rho, P) = \int HVI(P, y).PDF_{\mu,\sigma}(y)\, dy \quad (12)$$

Where, HVI denotes the improvement in the hypervolume of the Pareto front at the current iteration from adding a new training point, denoted as y, with μ and σ representing the parameters of the predictive distribution. Consequently, to maximize the Expected Hypervolume Improvement (EHVI) recalculation of the Gaussian Process posterior and sampling during each gradient step is required making it computationally intensive hence limiting the scalability in multi-objective optimization problems.

To solve the EHVI's computational demands, the qEHVI acquisition function was introduced, which generates q posterior samples from the Gaussian process (GP). For each sample point i, Si represents the region dominated by it but not by the current Pareto front P. The hypervolume improvement (HVI) from the q points is the Lebesgue measure as defined in [15] as in Eq.13

$$qHVI(\{x_i\} \forall\, i = 1 : q) = \varphi_k\left(U_{i=1}^{q} S_i\right) \quad (13)$$

Daulton et al. [15] proposed a Monte Carlo approximation for qEHVI by drawing N Sobol samples from the joint objective distribution and estimating qEHVI as the average qHVI across these samples as given in (Eq.14)

$$qHVI(\{x_i\} \forall\, i = 1 : q) \cong \frac{1}{N} \sum_{t=1}^{N} (qHVI) \quad (14)$$

B. Proposed Approach

This study formulates a dynamic optimization problem to determine the optimal C-rate for each predefined stage of a multi-stage charging protocol. The proposed methodology is outlined in the following pseudocode.

Algorithm: Pseudo code of optimal charging strategy

INPUT: N_init (initial sample size), **T** (BO iteration), **S** (number of stages), Bounds [(lb, ub)] for each C-rate stage, Objectives: [f_1, f_2, f_3], Constraints [g_1, g_2, g_3]

BEGIN:

Generate initial design of N_init C-rate using Sobol sampling

1.Initialization:

FOR each individual **x** in N_init:
Run SPMeT simulation with **x**, a vector of c-rates
Compute objective $f_1(x)$, $f_2(x)$, $f_3(x)$
Check constraints feasibility
Store initial Dataset D = {x, f(x), g(x)}

2. Surrogate Models:

Train Gaussian Process (GP) models for each (Objective and constraint)

3. Bayesian Optimization Loop (for t= 1 to T):

WHILE(t<=T)

-Use multi-objective acquisition function (qEHVI)
- Exploit GP predictions to propose next candidate
- Handle feasibility through probabilistic constraint Modelling
-Evaluate proposed candidates:
FOR each x in X_next:
Run SPMeT simulation
Compute $f_1(x)$, $f_2(x)$, $f_3(x)$
Compute constraint violation values
-Update dataset:
Add {(x, f(x), g(x))} to D

Termination criterion:

-Hypervolume(t)-Hypervolume(t-1) < 0.0001

OUTPUT:

- Final feasible Pareto front
-Corresponding Objective values [f_1, f_2, f_3]
- Corresponding Optimal C-rate values

V. Results and Discussion

In this section, we have discussed the results obtained by solving MOOP using a well-established evolutionary algorithm namely NSGA-II and the proposed Muti-Objective Bayesian Optimization to quantify the comparative benefits associated with them.

A. Multi-Objective Bayesian Optimization Solution

The SPMeT battery model was integrated with MOBO which was run with q-EHVI as acquisition function iteratively to generate results. MOBO was coded using BoTorch and NumPy packages. Fig.1 shows three 2D Pareto plots of the three objective optimization problem taking 2 objectives at a time using the q-EHVI acquisition function driven multi-objective Bayesian optimization. Each subplot clearly reveals a conflicting trade-off relationship among the objective functions (e.g. rise in temperature happens for fast charging but aim is to find fast charging protocols with less temperature rise; slow charging helps to store more charge but aim is to store more charge with fast charging etc.).

The qEHVI acquisition function explores wide range of region of the objective space during early iterations; however, as the optimization progresses, the samples rapidly converge toward the Pareto-optimal (PO) boundary. This confirms that qEHVI effectively balanced exploration of uncertain region with balanced exploitation of promising solution region.

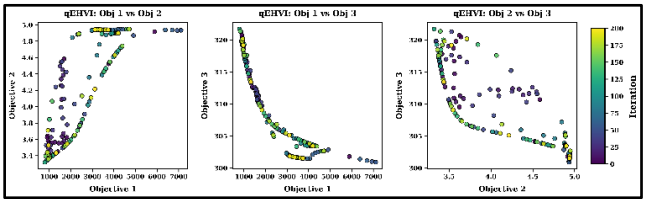

Fig 1. Pairwise visualisation of the three-objective optimisation results for q-EHVI-based MOBO.

As seen from Fig 2, the hypervolume steadily increases during initial iterations and becomes constant ~200th iteration, indicating q-EHVI was able to explore the non-dominant solution and converges towards the Pareto Front around 200 iterations. Fig 3 shows the evolution of PO fronts through 20th, 40th, 80th, 120th, 160th and 200th iterations, which becomes constant after 200th iteration.

Next, the multi-objective problem as discussed in section 2.2 was also solved using NSGA-II for 200 generation with population size of 50. The mutation and probability and cross-over probability were set to be 0.5 and 1.0 respectively.

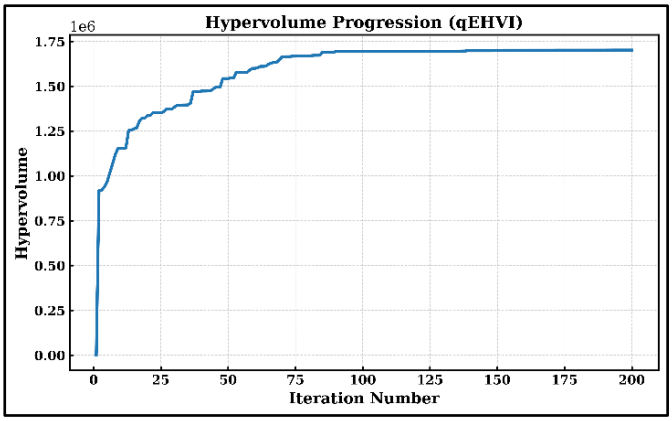

Fig 2. Plot showing hypervolume progressively increased with iteration.

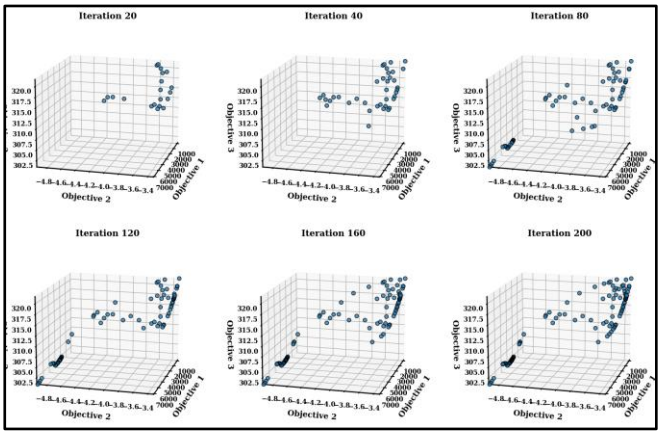

Fig 3. Plot showing evolution of Pareto fronts obtained from MOBO at different iterations.

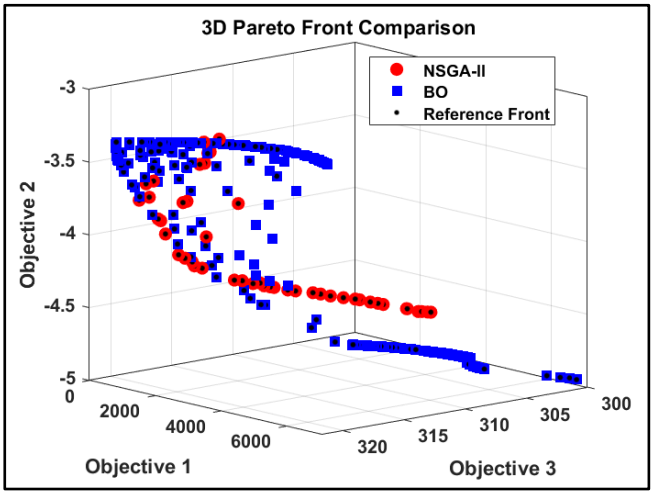

Fig 4. Pareto-front comparison for solutions obtained from NSGA-II and MOBO algorithms

Fig.4 shows the comparative analysis of PO fronts obtained using NSGA-II and MOBO along with a reference Pareto front which was obtained by performing non-dominant sorting on the combined solution from both the algorithms and retaining only the rank-1 solutions. The reference PO front is used as a benchmark for evaluating the convergence and diversity between the above-mentioned algorithms. A quantitative analysis was performed based on the performance metrices where MOBO demonstrates substantially improved convergence characteristics, achieving significantly lower inverse generational distance (IGD) value of 0.885 compared to NSGA-II (354.95), indicating closer alignment with the reference front. For PO solution diversity, spacing metric was found marginally lower for MOBO (23.54) than for NSGA-II (24.33), indicating uniform spread of PO solutions across the solution space. Additionally, MOBO achieves a notably higher diversity metric (DM = 0.936) relative to NSGA-II (DM = 0.650), demonstrating improved coverage and convergence across the objective space. This shows the PO front obtained by MOBO was marginally better or similar to that obtained by NSGA II based on both the convergence and diversity metrics, two pillars of performance metric comparison for multi-objective optimization algorithms. Next, we compared the number of function evaluations utilized by both the algorithms as mentioned in Table II. MOBO used 200 function evaluations with an additional 6 initial guesses and NSGA II used 10000 function evaluations while finding the final PO solutions. This shows the huge promise of MOBO, which can find PO solutions for the problem under consideration using only 2.06% of the function calls compared to NSGA II.

TABLE II. COMPARSION BETWEEN NSGA-II AND MOBO

Optimization algorithms	Hypervolume	Number of function calls
NSGA-II	1.6139e06	10000
BO	1.7120e06	200 + 6

B. Pareto Front Characterisation

As there are many solutions in the PO set for a multi-objective optimization problem, it is worth to find patterns among the them, with each having its individual characteristics of its own. To explore these characteristics, we performed Hierarchical clustering among the PO solutions based on their objective function values. Fig.5 presents a dendrogram plot obtained from Hierarchical clustering, clearly indicating four distinct clusters coming as solution.

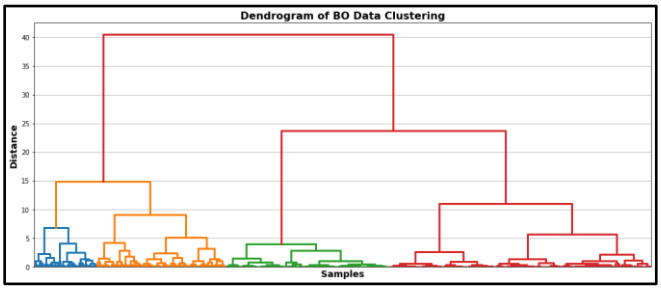

Figure 5. Hierarchical clustering dendrogram for the PO solutions

Since each cluster contains multiple solutions as seen in (Fig.4) we use statistical criteria, such Akaike Information Criterion (AIC) and Bayesian Information Criterion (BIC), to evaluate each solution and pick one among them based on the AIC and BIC score. Table III shows the selected 4 solution from each cluster. Negative C-rate values correspond to charging current. From the last column of the table, it is clear that solutions coming from each cluster has a different signature and purpose which can be further utilized while picking a single solution from the set of PO solutions based on the solution applications.

TABLE III. SELECTED PARETO SOLUTION BASED ON AIC/BIC CRITERION

Cluster	AIC	BIC	C-rate	Remark
1	9.093	22.72	[-2.54, -2.30]	Fast charging, high temperature
2	13.134	24.987	[-1.76, -1.32]	Moderate Charging
3	2.8101	19.627	[-1.787, -0.5]	Optimal charging time charge,
4	4.194	16.576	[-2.88,0.698]	Slowest charging

VI. CONCLUSION

This study develops an optimal charging framework for Li-ion batteries employing a detailed electrochemical model SPMeT. Consideration of such detailed physical model enables us to capture important electrochemical phenomena fairly accurately by leveraging the model fidelity. The proposed framework investigates the trade-offs among the conflicting objectives, i.e., charging time, final temperature and charge stored and Multi-objective Bayesian Optimization was utilized to find the Pareto optimal solutions. Unlike conventional gradient-based methods that risk convergence to local minima, BO builds surrogate models (e.g., using Gaussian Processes) to approximate the multi-objective Pareto space and iteratively refine the model in an adaptive fashion while migrating towards the set of optimal solutions. MOBO shows tremendous promise in finding similar quality PO solutions utilizing a fraction of function evaluations compared to NSGA II. After performing Pareto Front characterization using hierarchical clustering, the entire Pareto set is clustered into different groups to characterize the Pareto front structure and identify distinct regimes. Such classification provides critical insight into how operational priorities influence the choice of optimal charging profiles.

CONFLICT OF INTERREST

The authors declare that we have no known competing financial interests or personal relationships that could have appeared to influence the work reported in this paper.

REFERENCES

[1] S. M. Lukic *et al.*, “Energy Storage Systems for Automotive Applications,” vol. 55, no. 6, pp. 2258–2267, 2008.

[2] M. Usman Tahir, A. Sangwongwanich, D. I. Stroe, and F. Blaabjerg, “Overview of multi-stage charging strategies for Li-ion batteries,” *J. Energy Chem.*, vol. 84, pp. 228–241, 2023, doi: 10.1016/j.jechem.2023.05.023.

[3] H. E. Perez *et al.*, “Optimal Charging of Li-Ion Batteries via a Single Particle Model with Electrolyte and Thermal Dynamics Optimal Charging of Li-Ion Batteries via a Single Particle Model,” 2017, doi: 10.1149/2.1301707jes.

[4] F. Brosa and W. D. Widanage, “A Single Particle model with electrolyte and side reactions for degradation of lithium-ion batteries,” *Appl. Math. Model.*, vol. 121, pp. 586–610, 2023, doi: 10.1016/j.apm.2022.12.009.

[5] M. Doyle, T. F. Fuller, and J. Newman, “Modeling of Galvanostatic Charge and Discharge,” *J. Electrochem. Soc.*, vol. 140, no. 6, pp. 1526–1533, 1993.

[6] S. Zhang, C. Zhang, R. Xiong, and W. Zhou, “Study on the Optimal Charging Strategy for Lithium-Ion Batteries Used in Electric Vehicles,” no. 3, pp. 6783–6797, 2014, doi: 10.3390/en7106783.

[7] Z. Guo, B. Yann, X. Qiu, L. Gao, and C. Zhang, “Optimal charging method for lithium ion batteries using a universal voltage protocol accommodating aging,” *J. Power Sources*, vol. 274, pp. 957–964, 2015, doi: 10.1016/j.jpowsour.2014.10.185.

[8] S. Bashash, S. J. Moura, J. C. Forman, and H. K. Fathy, “Plug-in hybrid electric vehicle charge pattern optimization for energy cost and battery longevity,” *J. Power Sources*, vol. 196, no. 1, pp. 541–549, 2011, doi: 10.1016/j.jpowsour.2010.07.001.

[9] B. Jiang *et al.*, “Fast charging design for Lithium-ion batteries via Bayesian optimization,” *Appl. Energy*, vol. 307, no. July 2021, p. 118244, 2022, doi: 10.1016/j.apenergy.2021.118244.

[10] A. Abdollahi *et al.*, “Optimal battery charging, Part I: Minimizing time-to-charge, energy loss, and temperature rise for OCV-resistance battery model,” *J. Power Sources*, vol. 303, pp. 388–398, 2016, doi: 10.1016/j.jpowsour.2015.02.075.

[11] R. Zhu, W. Peng, F. Yang, and M. Xie, “Fast-Charging Protocols Design of Lithium-Ion Battery : A Multiple-Objective Bayesian Optimization Perspective,” *IEEE Trans. Transp. Electrif.*, vol. 11, no. 3, pp. 8327–8338, 2025, doi: 10.1109/TTE.2025.3539853.

[12] K. Wang and A. W. Dowling, “ScienceDirect Bayesian optimization for chemical products and functional materials,” *Curr. Opin. Chem. Eng.*, vol. 36, p. 100728, 2022, doi: 10.1016/j.coche.2021.100728.

[13] L. Shu, P. Jiang, X. Shao, and Y. Wang, “A New Multi-Objective Bayesian Optimization Formulation With the Acquisition Function for Convergence and Diversity,” vol. 142, no. September, pp. 1–10, 2020, doi: 10.1115/1.4046508.

[14] S. Daulton and M. Balandat, “Parallel Bayesian Optimization of Multiple Noisy Objectives with Expected Hypervolume Improvement,” no. NeurIPS, 2021.

[15] S. Daulton and M. Balandat, “Differentiable Expected Hypervolume Improvement for Parallel Multi-Objective Bayesian Optimization arXiv : 2006 . 05078v3 [stat . ML] 23 Oct 2020,” no. 1, pp. 1–30, 2020.